Along Stream Variations in Valley Flank Erosion Rates Measured Using 10Be Concentrations in Colluvial Deposits From Canyons in the Atacama Desert

Valeria Zavala, Sébastien Carretier, Vincent Regard, Stéphane Bonnet, Rodrigo Riquelme, Sandrine Choy

AGU ADVANCING EARTH AND SPACE SCIENCE

Geophysical Research Letters

RESEARCH LETTER
10.1029/2020GL089961

Key Points:

- Measurements of ^{10}Be concentrations in colluvial deposits quantify along-stream valley flank erosion rates
- Erosion rates consistently increase with the valley slope and decreases with the valley width
- An approach and a first data set for testing lateral erosion laws governing the valley widening rate

Supporting Information:

- Supporting Information S1
- Supporting Information S2

Correspondence to:
V. Zavala and S. Carretier,
valeria.zavala@get.omp.eu;
sebastien.carretier@get.omp.eu

Citation:
Zavala, V., Carretier, S., Regard, V., Bonnet, S., Riquelme, R., & Choy, S. (2021). Along-stream variations in valley flank erosion rates measured using ^{10}Be concentrations in colluvial deposits from canyons in the Atacama Desert. *Geophysical Research Letters*, *48*, e2020GL089961. https://doi.org/10.1029/2020GL089961

Received 12 AUG 2020
Accepted 21 JAN 2021

Along-Stream Variations in Valley Flank Erosion Rates Measured Using ^{10}Be Concentrations in Colluvial Deposits From Canyons in the Atacama Desert

Valeria Zavala[1], Sébastien Carretier[1], Vincent Regard[1], Stéphane Bonnet[1], Rodrigo Riquelme[2], and Sandrine Choy[1]

[1]Géosciences Environnement Toulouse (GET), Université de Toulouse, CNRS, Toulouse, France, [2]Departamento de Ciencias Geológicas, Universidad Católica del Norte, Antofagasta, Chile

Abstract The widening and deepening of river valleys occur at different rates. This co-evolution is largely undocumented over thousands of years. Uncertainties on incision and widening laws limit the ability of models to reproduce erosion rates and responses to tectonics and climate over geologic timescales. We studied two 1 km-deep canyons in northern Chile, both characterized by valley widening after the upward migration of a major knickzone but with a diachronous incision initiation. We use ^{10}Be concentrations measured in colluvial deposits to quantify the erosion rates E of along-stream valley flanks. We observe that E increases in the knickzone, with well-defined relationships ($R2 = 0.7$): E increases quasilinearly with the valley-bed slope and decreases with the valley width (exponent ~-0.4). Our results suggest that E decreases with time but that valley flank weathering may sustain a significant lateral erosion rate. Our results provide data for testing erosion laws governing valley widening.

Plain Language Summary A common feature of river landscapes is the widening of valleys downstream (i.e., floodplains). Several studies have explored valley width controls, considering that different processes can control it, such as lithology and river hydraulic variations downstream. However, little is currently known about how the widening of valleys, in particular, occurs. To understand these processes, we studied two 1 km-deep canyons in northern Chile, both characterized by a different valley width downstream, a sharp change in valley slope (or knickzone), and different timings for the beginning of the incision. In an original way, we measured the concentrations of ^{10}Be in the colluvial deposits at the foot of the valley flanks to quantify the rate at which the flanks are eroded at different locations along the valley. Our results show that the erosion rates increase toward the knickzone, given that they are positively correlated with the slope of the valley floor and they decrease as the valley width increases. Our results suggest that the widening rate decreases with time but that the concomitant weathering of the valley flanks favors their lateral erosion. Our results give confidence in this new approach and provide the first data set to test the existing valley widening laws.

1. Introduction

Due to the tree structure of drainage networks, the amount of water flowing in streams increases downstream, which is accommodated by a change in water velocity and/or in channel geometry such as the river width-to-depth ratio. An empirical relationship between river width and water discharge (Q_w) is observed (Leopold & Maddock, 1953). The variation in bedrock river width with a changing Q_w or uplift rate has been a research focus over the last 20 years, because the river width adaptation controls the incision rate and thus the landscape response to climate and tectonic variations (Amos & Burbank, 2007; Bufe et al, 2016, 2019; Croissant et al., 2019; Hartshorn et al., 2002; Lavé & Avouac, 2001; Turowski et al., 2009; Whittaker et al., 2007; Yanites & Tucker, 2010). However, with the exception of some gorges (Barbour et al., 2009; Cook et al., 2014; Hartshorn et al., 2002), valleys are usually wider than their rivers since channels move and erode laterally. Yet, factors controlling the rate of valley widening by lateral erosion are poorly understood.

Valley widening occurs by occasional contacts between river channels and valley flanks (Hancock & Anderson, 2002). Thus, the valley widening rate depends on erosion processes acting at the scale of the channel bank itself and on processes controlling the lateral mobility of river channels on the valley floor.

At the scale of a bedrock river channel bank, field and experimental studies suggest that lateral erosion is decoupled from the incision of the river (Cook et al., 2014; Johnson & Finnegan, 2015). This potential decoupling is linked to several phenomena. For clay-rich lithologies, the alternation of wetting and drying periods physically alters the banks, increases their erodibility and favors lateral erosion over vertical incision. Lateral erosion may thus be favored by variations in water discharges (Johnson & Finnegan, 2015; Montgomery, 2004; Schanz & Montgomery, 2016; Stock et al., 2005). In addition, when the sediment supply increases, the river bed may be protected from vertical incision (cover effect), thereby promoting bank erosion (Baynes et al., 2020; Beer et al., 2017; Hartshorn et al., 2002; Lague, 2010; Li et al., 2020), although the role of sediment discharge may vary (Bufe et al., 2019; Cook et al., 2014). The macro-roughness of the river bed also plays a role by deflecting the trajectory of coarse bedload particles that impact and erode river banks (Finnegan et al., 2007; Fuller et al., 2016; Li et al., 2020; Turowski, 2020). Conversely, bank height may limit bank erosion (Bufe et al., 2019). Vegetation is known to increase the cohesion and to limit the erosion of channel banks (Vargas-Luna et al., 2019), to slow down the lateral mobility of meanders (Lelpi & Lapotre, 2020), and to increase the minimum stress that needs to be overcome in order to detach blocks from the flanks (Langston & Temme, 2019).

At the scale of a valley, widening processes are more difficult to address because they involve discrete contact events over long timescales (>1 kyr), for which the frequency and magnitude of the effects are largely unknown. It is likely that the factors that promote the lateral shift of rivers also promote valley flank erosion. As an example, Stark et al. (2010) show that the sinuosity of meandering rivers increases with increasing discharge variability, which then appears as a potential control of flank erosion in this specific case. Similarly, high sediment and water discharges may promote a higher lateral mobility of rivers (Bufe et al., 2016; Constantine et al., 2014; Wickert et al., 2013) and thus likely increases the probability of their contact with the valley flanks. Conversely, sediment input coming from the valley flanks themselves may inhibit lateral erosion if this input is higher than the transport capacity of the rivers (Malatesta et al., 2017). The efficiency of these processes to widen a valley depends on the nature of the rocks that compose the eroded bedrock (Brocard & der Beek, 2006; Langston & Temme, 2019). This complexity makes it difficult to establish a parametrical model for valley widening.

Nevertheless, Hancock and Anderson (2002) proposed a numerical model of lateral planation that considers a probability of contact between the river and its valley flank that only depends on the channel-to-valley width ratio. This model thus predicts that the widening rate of valleys decreases with time as they widen because of the progressive reduced likelihood of contacts between the river and its valley flanks. This decrease is also seen in flume experiments on bedrock channels with a fixed base-level, due to the decrease in sediment transport capacity and shear stress exerted on the river bed and banks as the river widens (Fuller et al., 2016; Limaye, 2020). In experiments with a base-level fall (Schumm et al., 1987), widening occurs after a first incision phase driven by the upstream propagation of a knickpoint, and then widening rate decreases with time until the valley width has reached a steady-state value (Schumm et al., 1987). By studying canyons carved into the Tian Shan alluvial piedmont, Malatesta et al. (2018) proposed a similar scenario, in which widening is first impeded by higher valley flanks, but then dominates when the vertical incision subsequently stalls. Mouchene et al. (2017) modeled the autogenic incision of the Pyrenean piedmont using a lateral erosion rate proportional to the sediment discharge. Their model also predicts that, after incision, valleys widen at a decreasing rate.

Finally, studies that have investigated valley widening processes have often looked for relationships between valley width W_V and drainage areas (a proxy for discharge), similar to those accounting for river width (Brocard & der Beek, 2006; Langston & Temme, 2019; Leopold & Maddock, 1953; May et al., 2013; Schanz & Montgomery, 2016; Tomkin et al., 2003). The exponent of the valley width-area power law relationship is generally larger than the river width one (May et al., 2013; Tomkin et al., 2003), indicating that the valley width increases more rapidly than the channel width, for reasons that have not yet been demonstrated. Landscape evolution models that have included different lateral erosion laws predict an equilibrium W_V scaling as $Q_w^{0.3-0.5}$ (Carretier et al., 2016; Langston & Tucker, 2018), which is consistent with several observations (Brocard & der Beek, 2006). This relationship does not seem to discriminate the lateral erosion law.

This nonexhaustive review illustrates the ambiguous effects of certain factors such as water and sediment discharges on the valley widening rate, potentially because they are not independent and they both act at

the channel bank and valley floor scale over different periods. A large part of the uncertainty on the lateral erosion law relies on the lack of a method to quantify the valley widening rates averaged over periods that integrate the variability of river processes. Here, we take advantage of the relatively simple geometry of two Andean canyons incising an Oligo-Miocene surface in northern Chile. They present transient stages of evolution through knickzone retreat, with different degrees of deepening and widening downstream (Figure 1). We use cosmogenic ^{10}Be concentrations in the colluvium at the foot of hillslopes in these canyons to estimate the valley flank erosion rate (E). Our aim is to verify the applicability of this approach so as to explore how E varies downstream from the knickzones as the valleys widen and deepen. Here, the flank is defined as the hillslope between the valley floor and a summit surface incised by the canyons. The ^{10}Be concentration measured in riverine sediment is frequently used to estimate average millennial catchment-wide erosion rates, by assuming that the concentrations were derived only from in-situ ^{10}Be on hillsides (Portenga & Bierman, 2011). Our approach is similar, but we use the ^{10}Be concentration in colluvium sediment instead of river sediment to record the average erosion rate in their source area, corresponding to a small portion of the valley flank along the valley.

2. Study Area

The Chiza and Tana canyons, 0.5–1 km deep (Garcia et al., 2011; Hoke et al., 2007; Schlunegger et al., 2006), are located on the western slope of the Central Andes (Figure 1). Their incision occurs through the eastward migration of a knickzone in response to a Miocene surface uplift of the forearc, with diachronous onsets of canyon incision along the coast, and a mean knickzone migration rate on the order of 1–5 km/m.y (Garcia et al., 2011). An arid to hyperarid climate prevails, with precipitation that increases on average from $<$ 10 mm/yr in the Coastal Cordillera (CC) toward 100 mm/yr in the Western Cordillera (WC) (Garreaud et al., 2010). These two canyons progressively widen downstream from a knickzone located roughly 50 and 25 km from the coast in the Chiza and Tana canyons (Figures 1d and 1e). Another steeper knickzone is found roughly 50 km further upstream in the Chiza Canyon, but is not included in the analysis (Figure 1d). The headwaters of these two rivers, several tens of kilometers away, are found in the WC. They flow to the Central Depression (CD) before incising the Coastal Cordillera and reaching the Pacific Ocean (Figure 1a). In the CD, the Chiza and Tana valleys dissect an extensive, gently westward-dipping erosional surface corresponding to the top of Oligo/Miocene volcano-sedimentary rocks (Oxaya and El Diablo Fm.; Figures 1d and 1e). The canyon incision started at 11 Ma in Chiza based on the minimum age of the upper deposits of the CD (Garcia et al., 2011). The incision of the Tana Canyon probably initiated more recently, approximately 3 Myr ago, as evidenced by the presence of a paleolake located on the western side of the CD and incised by the Tana River (Figure 1a). This paleolake likely acted as a local base level for the upstream Tana drainage until its abandonment at ∼3 Ma (Kirk-Lawlor et al., 2013). The Chiza and Tana catchments have comparable drainage areas but the knickzone distance from the outlet as well as the valley width are smaller in Tana compared to Chiza. As a result, Tana can be considered as being at a less advanced transient stage compared to Chiza (Garcia et al., 2011). In the investigated area of the two canyons, the bedrock changes along-stream from the poorly cohesive El Diablo formation to the cohesive volcano-sedimentary Oxaya formations and then to dioritic intrusive rocks (basement; Figure 1) near the coast. El Diablo appears more erodible, while it is uncertain if a difference in erodibility exists between the Oxaya formation and the intrusive rocks. Both canyons have wide bedrock valley flanks partially covered by a regolith that becomes patchy near the knickzones. Their valley floors are covered by coarse sediment (sand to boulders) except in some portions of the narrowest gorges in Tana where, according to our field observations, the bedrock outcrops.

3. Methodology

The geometric features of the Tana and Chiza canyons have been measured using 30-m resolution DEM from NASA's Shuttle Radar Topography Mission (Farr et al., 2007). The canyons show linear valley flank cross-sectional profiles downstream from their main knickzone (Figure S1), whereas the flanks are more convex upstream. In both canyons, the transition from valley flank to valley floor is clearly defined by a break in the slope that was used to delineate the valley floor margins and to define a valley centerline, along which the elevation profile and valley bed slope (S_V) and width (W_V) were measured. The valley flank slope (S_F) was calculated by using a linear fit on elevation data along 120 profiles (spaced at roughly every 0.5 km

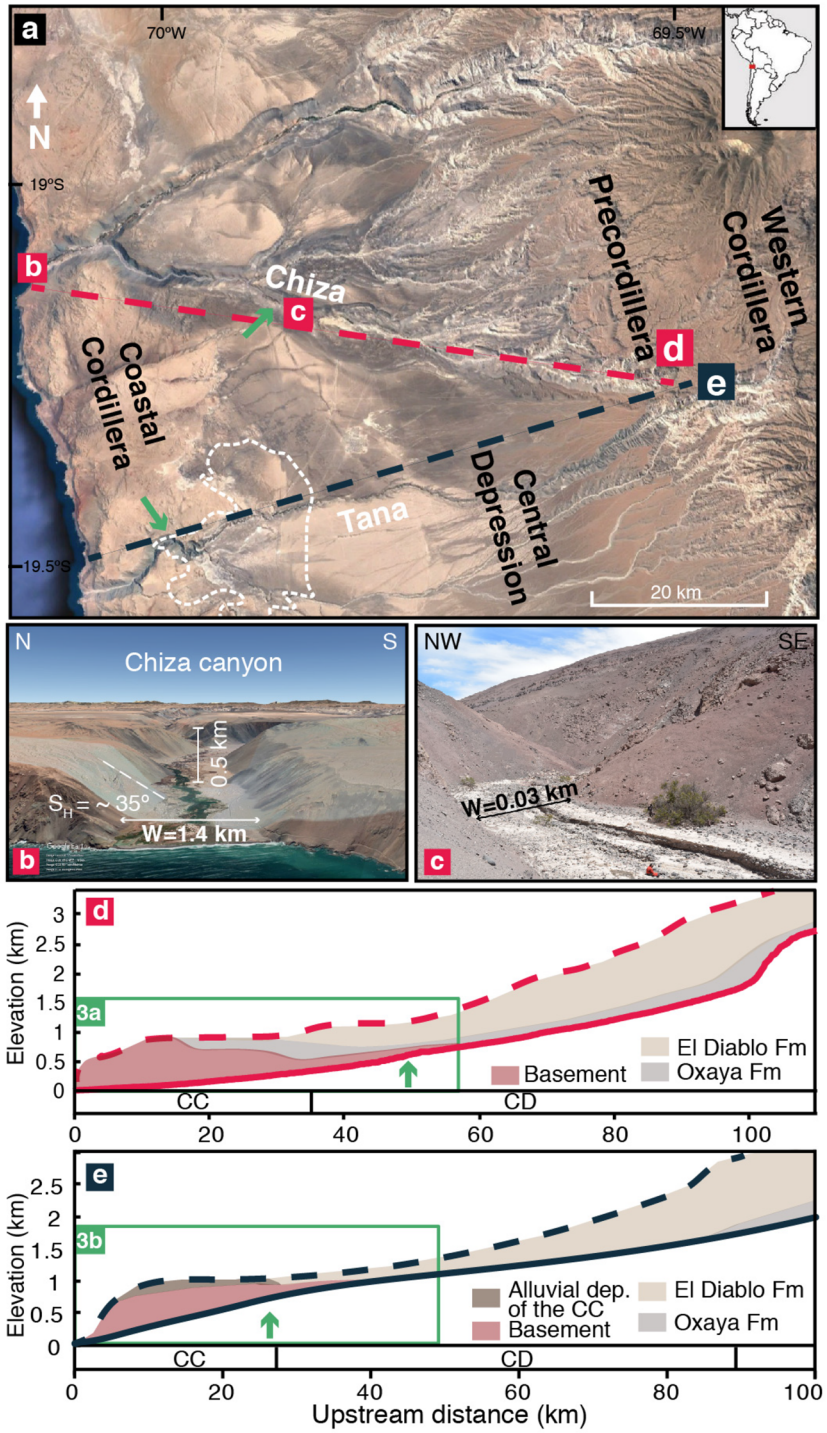

Figure 1. (a) Image (Google Earth™) of the Central Andes in northern Chile showing the four morphotectonic units and the Tana paleolake boundaries (dotted white line) (Kirk-Lawlor et al., 2013). The green arrows indicate the considered knickzone in each canyon. (b) Image of the mouth of the Chiza River (Google Earth™). (c) Field photo of Chiza Canyon near its knickzone. D and (e) Paleosurfaces (dashed lines) and longitudinal river profiles (solid line) of the Chiza and Tana canyons, respectively. Cross-section based on the geological map from SERNAGEOMIN along canyon hillsides (García et al., 2013; García & Fuentes, 2012). It shows the schematic stratigraphic relationship between the basement outcrops, Oxaya Formation and El Diablo Formation. In both cases, the canyon flanks are covered by a layer of colluvium (as shown in c) that varies in thickness and prevalence. The green rectangle frames the downstream 50 km-long segment of the valleys where we measured the canyon features displayed in Figure 3.

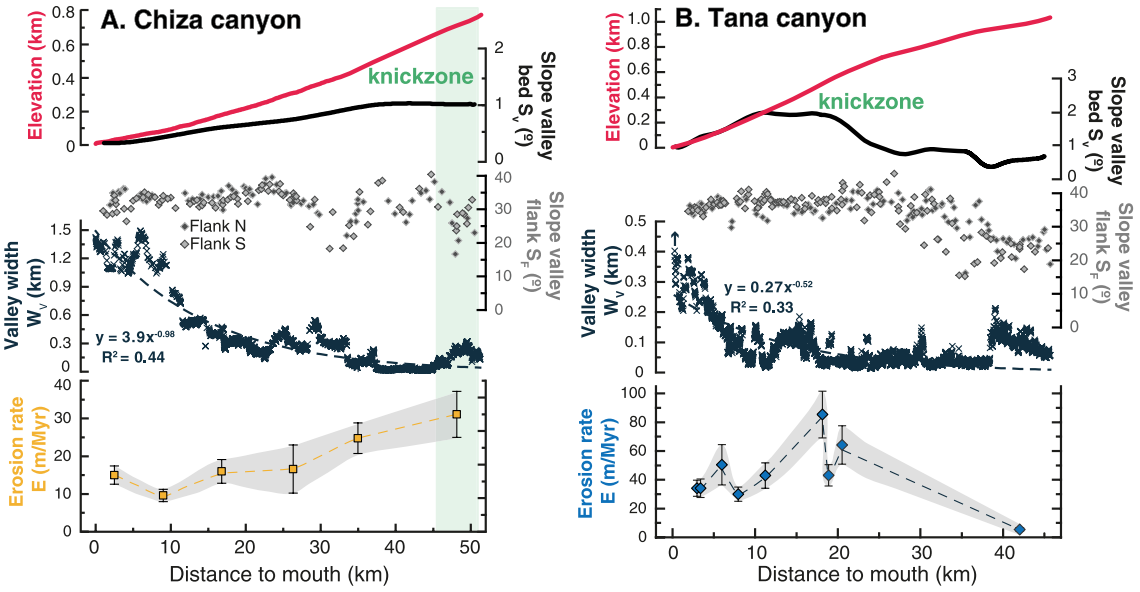

Figure 2. Features of the Tana and Chiza canyons: elevation profile, valley bed slope (S_V), valley flank slope (S_F), valley width (W_V) and hillside erosion rate (E). The location of the measurements is shown in Figures 1d and 1e. The canyon geometries were measured using 30-m resolution data from NASA's Shuttle Radar Topography Mission (Farr et al., 2007). The error bars for E represent the uncertainty in the measured ^{10}Be concentration and ^{10}Be production rates. The green rectangles show the upstream limb of the knickzones.

and parallel to the flow line direction) for each canyon flank. We used ^{10}Be concentrations from coarse sand (0.5–1 mm grain size) sampled in colluvium at the foot of the valley flanks along the canyons to estimate the mean local flank erosion rate (E) (Figures S2 and S3; See Supporting information for a description of the methodology), by assuming that the ^{10}Be concentration is representative of the production in the area upslope (Brown et al., 1995; Granger et al., 1996). It is essentially the same approach as the one extensively used to estimate catchment-wide erosion rates, however it is applied here for the first time to a portion of a valley flank. In this setting, fewer deviations from the method assumptions are likely to occur compared to river systems (imperfect mixing at confluences, episodic inputs by deep landslides, cosmogenic production during river transport; Yanites & Tucker, 2010).

To ensure that it represents the entire valley flank (from top to bottom above the sampling point), each sample contains five subsamples (~100 g) mixed together, collected along a ~50 m long line at the foot of the hillslopes, away from active channels at the time of sampling (November 2017—Figure S2). We determined the ^{10}Be production rate by calculating it on each pixel of an upslope contributing area determined with a flow routing algorithm on the hillslopes (see Figure S4 and Supplementary Information S1 for details). Taking into account a topographic shielding, this correction only changes E by a few % (Table S1). In the following, we will only consider the erosion rates calculated without a topographic correction as recommended by DiBiase (2018).

4. Results

In the two canyons, the valley bed slope S_V regularly decreases downward from the knickzone to the river mouth (Figure 2). In Tana Canyon, S_V also decreases upstream from the knickzone as the valley profile changes from concave to convex. The valley width W_V strongly increases for the two canyons downstream from their knickzones (Figure 2), reaching a maximum value of ~1.5 km in Chiza and ~0.4 km in Tana, i.e. roughly five-fold their width above the knickzones. Upstream from the knickzones, W_V is narrow (<100 m) and several kilometer-deep landslides (Figure S5) locally influenced the valley widths; this phenomenon is not investigated here because such huge landslides are not observed in our investigated area downstream.

Both canyons show power-law relationships between the valley width and drainage area with exponents of 1.59 and 1.58 for the Chiza and Tana valleys respectively, with large data dispersions (Figure S6). These

exponents are significantly larger than the commonly observed exponents, which are classically within the 0.3–0.5 range (Montgomery & Gran, 2001), probably due to the transient stage of the studied canyons. In Chiza Canyon, a step in the valley width occurs approximately 10 km upstream from the shoreline, at the confluence between the studied valley and the Camarones Valley. In Tana Canyon, a confluence with a hanging valley is located near the knickzone to the south of the main reach. The valley width significantly increases downstream from this confluence and the knickzone.

Downstream from the knickzones, the flanks of canyons show a nearly linear profile (Figures 1b and S1) with a constant S_F value close to 35° all along the canyons (Figure 2), close to the angle of repose for dry sand (Al-Hashemi & Al-Amoudi, 2018). Here, the canyon flanks are regolith-mantled and covered by mm to cm clasts, forming debris-wedges at their base, and occasionally showing bare bedrock exposure (Figure S2).

The cosmogenic-derived E values, between 9.8 ± 1.7 and 85.9 ± 16.6 m/Ma (Table S1), are in the range of the known values for steep slopes in the Atacama Desert (Carretier et al., 2018) and are of the same order of magnitude as the known catchment mean erosion rates in this area (Carretier et al., 2018; Starke et al., 2017). In Chiza Canyon, E increases upward from 9.8 ± 1.7 m/Ma near the river mouth to 31.2 ± 6.1 m/Ma near the knickzone (Figure 2). Similarly, in Tana Canyon, E increases upward from 34.9 ± 5.7 to 85.9 ± 16.6 m/Ma at the knickzone and then decreases to 5.5 ± 1.2 m/Ma upstream. We performed a repeatability test in Tana by measuring two samples on opposite sides of the 1.4 km-wide valley near its mouth. We obtained undistinguishable ^{10}Be concentrations (samples QTT05 and QTT06, Table S1), which supports our approach.

The whole data set shows that E broadly increases with S_F (Figure 3a), with a large dispersion of the data for increasing S_F, as has also been observed in numerous studies, where the erosion rate increases and varies dramatically near the gravitational stability slope (Carretier et al., 2013; Ouimet et al., 2009). Yet, the dispersion of E around S_F suggests that other factors likely influence E. We observe a better correlation between E and S_V (Figure 3b): higher E values are measured for higher S_V values, near the knickzones. Last, our data also indicate an inverse relationship between E and W_V (Figure 3c) and a co-variation of E with W_V and S_V (Figure 3d).

5. Discussion and Conclusions

To quantify the valley flank erosion rates, we assumed steady-state ^{10}Be concentrations over an integration timescale on the order of 1 m/E (Lal, 1991), that is, in the range 10–100 ka. During this period, the sea level dropped ~120 m in several steps between ~125 ka and the Last Glacial Maximum (LGM) ~25 ka ago. This drop in sea-level potentially accelerated the erosion near the river mouths of the investigated canyons. To estimate this potential bias, we modeled several scenarios of erosion acceleration between −125 and −25 ka (Figure S8). In the more realistic scenario, where we assume that the valley flanks erode at a slower rate than the sea level drop, the bias is on the order of the uncertainty for the ^{10}Be production rate (20%). As this bias is not spatially homogeneous but is expected to decrease from the coast upward, its effect would be to weaken the observed upstream increase in E. Considering a much larger bias (>100%), E would even decrease upward from the coast, contrary to what we observe for the two canyons.

Similarly, we found that the erosion rate variation associated with the knickzone retreat is not recorded in the ^{10}Be concentrations, as the retreat rate is slow enough (~1–5 km/Ma) to allow the ^{10}Be concentrations to equilibrate with the erosion rates (Figure S9).

Another potential bias concerns valley width near outlets. During the low stand of the LGM, rivers may have carved a narrower valley, now buried by postLGM aggradation. Unfortunately, there is no available data on the sediment thickness in these canyons. In the worst case (incision of 120 m below the current valley floors with constant S_F at depth) the buried valley floor near the outlet would be 22% narrower in Chiza and 100% in Tana. If true, this effect would then have only a minor influence on the Chiza data set and would not significantly change the trends observed in Figures 2 and 3. However, we cannot rule out that the potential W_V overestimation does not have a major influence on the Tana data. But in that case, the consistency between both datasets (Figure 3) would only be a coincidence, something that we consider to be unlikely. Moreover, as discussed above, E should decrease upstream in that case, contrary to what is

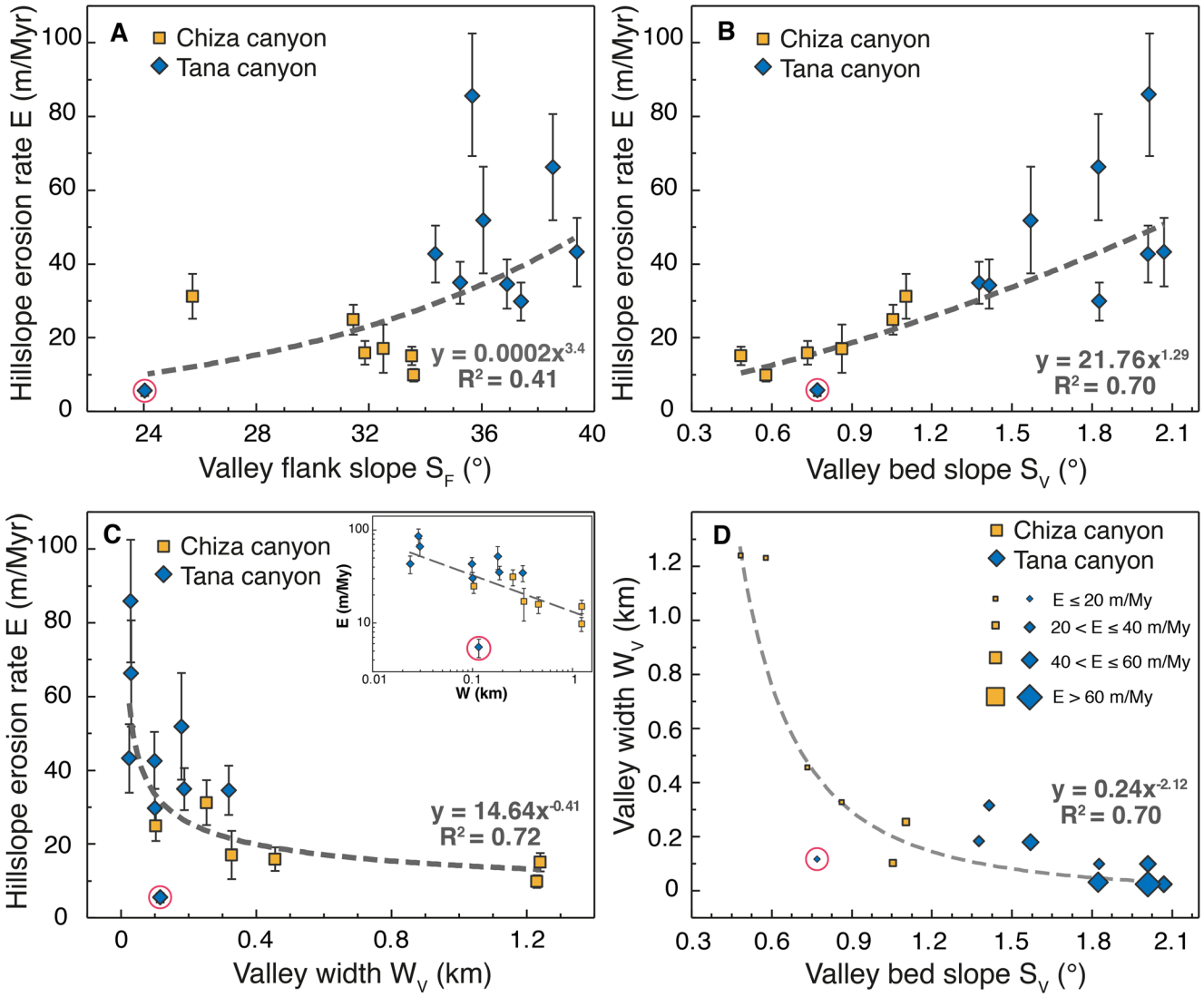

Figure 3. Relationship between the valley flank erosion rate (E) and: (a) Valley flank slope (S_F), (b) Valley bed slope (S_V), and (c) Valley width (W_V). In C the inset shows data in q logarithmic plot. (d) Relationship between W_V and the valley bed slope (S_V). The size of symbols is according to E. In all of the figures, the circle indicates the data point located upstream the Tana knickzone.

observed. Then, we believe that this end-member scenario is unrealistic and that the overestimation of the valley width due to the valley aggradation only has a minor influence in our data set.

Part of the material incised by the rivers consists of sediments from the uppermost El Diablo formation. Madella et al. (2018) showed that these sediments could contain an inheritance of roughly 10^4 atoms/g of ^{10}Be. In the Tana Valley, our ^{10}Be concentrations are greater than or equal to these concentrations. Two samples taken on two sides of the Tana Valley at the same distance from the outlet, with different thicknesses of the El Diablo sediments, yield the same concentrations (QTT05 and QTT06: Table S1), suggesting that the inheritance of this formation does not significantly bias our erosion rates. In the Chiza Valley, the ^{10}Be concentrations are one order of magnitude higher, well above the inheritance value reported by Madella et al. (2018).

Finally, shallow landslides and mass wasting on the studied valley flanks may generate imperfect mixing during the transfer of the materials on the hillslopes as well as time variations in the ^{10}Be concentrations at the sampling points. Nevertheless, the consistent spatial pattern of E (Figure 2), the same ^{10}Be

concentrations in the two samples located on opposite sides of the Tana Valley and the correlations of E with geomorphic parameters (Figure 3) suggest a minor effect of shallow landslides on our estimate of the erosion rates.

Several studies have linked the evolution of canyons in the western Central Andes to the retreat of knickzones (Abbuehl et al., 2011; Garcia et al., 2011; Schildgen et al, 2007, 2010; Schlunegger et al., 2006; Trauerstein et al., 2013). Along the Tana and Chiza canyons, the deepening induced by the knickzone retreat drives the formation of steep linear valley flanks. Our data show that E is at its maximum for narrow valleys, near the retreating knickzone, and progressively decreases downward as S_V decreases and the valley widens, as observed in experiments performed on rivers responding to a base-level fall (Schumm et al., 1987).

An original aspect of our study is the potential link between valley width and flank erosion rates. Despite the potential bias discussed above, whole datasets exhibit clear inverse relationships between E and W_V (Figure 3c) following a power law with an exponent of ∼-0.4. We consider the possibility that this correlation is not a causal relationship, as W_V is inversely correlated with S_V, which is itself correlated to E (Figure 3). Nevertheless, our estimated E includes a vertical incision rate component, and a lateral erosion rate component (Fig. S10). Part of the erosion rate of the valley flanks is likely the result of lateral erosion caused by single or multiple channels as they wander across the floodplain due to avulsion or bank erosion, given that the contact between a river and its flanks is a necessary condition for a valley to widen (Hancock & Anderson, 2002). This view is supported by our field observations of the recent activation of hillslope debris where channels were in contact with the valley flanks. The measured erosion rate is therefore not only the result of the incision rate, controlled by S_V, but also of the widening rate of these valleys via the lateral erosion of the rivers. The vertical incision rate likely controls the valley flank erosion rate E in the knickzones, where the channel and valley widths are very similar. Conversely, near the valley mouths, far downstream from the knickzones, we can assume that the lateral erosion rate dominates over the incision rate and that the valley lateral erosion rate is close to E. Without an independent quantification of the vertical incision component, it is not possible to estimate the longitudinal variation of the lateral erosion rate without more details here. With this limitation in mind, we discuss the previous findings in light of our results.

Following the concept developed by Hancock and Anderson (2002), we hypothesize that the widening rate of the Chiza and Tana valleys is controlled by the frequency of the episodic contacts between the channels and their valley flanks. In addition to a predicted decrease in the incision rate downstream from the knickzone, part of our observed downstream decreasing trends in the flank erosion rates may be explained by the decreased probability for channels to be in contact with their flanks in wide valleys. This negative effect of valley width is supported by the smaller E in Chiza than in Tana near their outlets (where E is close to the lateral erosion rate).

Our data do not show clear evidence that valley widening is limited by valley flank height (Malatesta et al., 2017) (Figure S11). Lateral erosion seems to be efficient enough to remove the sediments supplied from the eroding valley flanks, and to maintain their slope close to 35° during the widening process. We can speculate that as E decreases downward, the conversion of bedrock to more erodible regolith may favor lateral erosion, which may partly counterbalance the reduced probability of contact between an active stream and the valley flanks. This positive role of weathering at the valley scale could broaden previous findings about physical weathering of river banks (Montgomery, 2004).

If true, lateral channel mobility and weathering over a millennial timescale should be key for understanding the geometry of the Chiza and Tana canyons and their erosion rates, which requires further research. In particular, the evaluation of the relative impacts of water and sediment discharges requires an independent estimate of the vertical incision rate. Therefore, we consider our study to be a first step toward this in that it provides a new tool. Given the lack of knowledge on valley widening laws in landscape evolution models, our datasets may constitute a unique benchmark for testing numerical models on the geometric evolution of valleys.

Our results suggest that it is possible to document the long-term erosion rate of canyon flanks using cosmogenic nuclides in colluvium. This approach is different from taking sediment within the river, which can only be used to quantify the erosion rate of nested catchments, and provides a more local erosion rate

averaged over periods that integrate the contributions of all erosive events. We anticipate that repeating this approach in other simple canyons may provide new clues on transient river deepening and widening, something that is much needed in order to test models.

Data Availability Statement

Data sets for this research are available in the Supporting Information and in this data repository: https://doi.org/10.26022/IEDA/111860

Acknowledgments
Valeria Zavala thanks the Agencia Nacional de Investigación y Desarrollo (ANID- Chile) through the PhD funding Scholarship Program "DOCTORADO BECAS CHILE/2015–72160597". This study was also funded by CNRS-INSU (project "Incision Chili") and by IRD through the LMI COPEDIM. The authors thank Luca Malatesta and Aaron Bufe for their constructive and helpful reviews.

References

Abbuehl, L. M., Norton, K. P., Schlunegger, F., Kracht, O., Aldahan, A., & Possnert, G. (2011). Corrigendum: El Nino forcing on ^{10}Be-based surface denudation rates in the northwestern Peruvian Andes? (vol 123, pg 257, 2010). *Geomorphology*, *129*(3–4), 417. https://doi.org/10.1016/j.geomorph.2011.02.023

Al-Hashemi, H. M. B., & Al-Amoudi, O. S. B. (2018). A review on the angle of repose of granular materials. *Powder Technology*, *330*, 397–417. https://doi.org/10.1016/j.powtec.2018.02.003

Amos, C., & Burbank, D. (2007). Channel width response to differential uplift. *Journal of Geophysical Research.*, *112*(F2), F02010. https://doi.org/10.1029/2006JF000672.

Barbour, J., Stark, C., Lin, C.-W., Chen, H., Horng, M.-J., Ko, C.-P., et al. (2009). Magnitude-frequency distributions of boundary shear stress along a rapidly eroding bedrock river. *Geophysical Research Letters*, *36*(4). https://doi.org/10.1029/2008GL035786

Baynes, E. R., Lague, D., Steer, P., Bonnet, S., & Illien, L. (2020). Sediment flux-driven channel geometry adjustment of bedrock and mixed gravel-bedrock rivers. *Earth Surface Processes and Landforms*. https://doi.org/10.1002/esp.4996

Beer, A. R., Turowski, J. M., & Kirchner, J. W. (2017). Spatial patterns of erosion in a bedrock gorge. *Journal of Geophysical Research: Earth Surface*, *122*(1), 191–214. https://doi.org/10.1002/2016JF003850

Brocard, G., & der Beek, P. V. (2006). Influence of incision rate, rock strength and bedload supply on bedrock river gradients and valley-flat widths: Field-based evidence and calibrations from western Alpine rivers (SE France). In S. D. Willett, N. Hovius, M. T. Brandon, & D. Fisher (Eds.), *Tectonics, climate and landscape evolution*. Geol. Soc. Am. Spec. Publ.

Bufe, A., Paola, C., & Burbank, D. W. (2016). Fluvial beveling of topography controlled by lateral channel mobility and uplift rate. *Nature Geoscience*, *9*(9), 706.

Bufe, A., Turowski, J. M., Burbank, D. W., Paola, C., Wickert, A. D., & Tofelde, S. (2019). Controls on the lateral channel-migration rate of braided channel systems in coarse non-cohesive sediment. *Earth Surface Processes and Landforms*, *44*(14), 2823–2836. https://doi.org/10.1002/esp.4710

Carretier, S., Martinod, P., Reich, M., & Goddéris, Y. (2016). Modeling sediment clasts transport during landscape evolution. *Earth Surface Dynamics*, *4*, 237–251. https://doi.org/10.5194/esurf-4-237-2016

Carretier, S., Regard, V., Vassallo, R., Aguilar, G., Martinod, J., Riquelme, R., et al. (2013). Slope and climate variability control of erosion in the Andes of central Chile. *Geology*, *41*(2), 195–198. https://doi.org/10.1130/G33735.1

Carretier, S., Tolorza, V., Regard, V., Aguilar, G., Bermudez, M. A., Martinod, J., et al. (2018). Review of erosion dynamics along the major N-S climatic gradient in Chile and perspectives. *Geomorphology*, *300*, 45–68. https://doi.org/10.1016/j.geomorph.2017.10.016

Constantine, J. A., Dunne, T., Ahmed, J., Legleiter, C., & Lazarus, E. D. (2014). Sediment supply as a driver of river meandering and floodplain evolution in the amazon basin. *Nature Geoscience*, *7*(12), 899.

Cook, K. L., Turowski, J. M., & Hovius, N. (2014). River gorge eradication by downstream sweep erosion. *Nature GeoSciences*, *7*(9), 682–686. https://doi.org/10.1038/NGEO2224

Croissant, T., Lague, D., & Davy, P. (2019). Channel widening downstream of valley gorges influenced by flood frequency and floodplain roughness. *Journal of Geophysical Research: Earth Surface*, *124*(1), 154–174. https://doi.org/10.1029/2018JF004767

DiBiase, R. A. (2018). Increasing vertical attenuation length of cosmogenic nuclide production on steep slopes negates topographic shielding corrections for catchment erosion rates. *Earth Surface Dynamics*, *6*(4). 923–931. https://doi.org/10.5194/esurf-6-923-2018

Farr, T. G., Rosen, P. A., Caro, E., Crippen, R., Duren, R., Hensley, S., et al. (2007). The shuttle radar topography mission. *Reviews of Geophysics*, *45*(2). https://doi.org/10.1029/2005RG000183.

Finnegan, N. J., Sklar, L. S., & Fuller, T. K. (2007). Interplay of sediment supply, river incision, and channel morphology revealed by the transient evolution of an experimental bedrock channel. *Journal Geophysical Research*, *112*(F3). https://doi.org/10.1029/2006JF000569

Fuller, T. K., Gran, K. B., Sklar, L. S., & Paola, C. (2016). Lateral erosion in an experimental bedrock channel: The influence of bed roughness on erosion by bed load impacts. *Journal of Geophysical Research: Earth Surface*, *121*(5), 1084–1105. https://doi.org/10.1002/2015JF003728

García, M., & Fuentes, G. (2012). Carta Cuya, Regiones de Arica y Parinacota y de Tarapacá. Servicio Nacional de Geología y Minería. Carta Geológica de Chile. *Serie Geología Básica*, *146*, 80.

García, M., Fuentes, G., & Riquelme, F. (2013). Carta Miñimiñi, Regiones de Arica y Parinacota y de Tarapacá. Servicio Nacional de Geología y Minería. Carta Geológica de Chile. *Serie Geología Básica*, *157*, 49.

Garcia, M., Riquelme, R., Farías, M., Hérail, G., & Charrier, R. (2011). Late Miocene-Holocene canyon incision in the western Altiplano, northern Chile: Tectonic or climatic forcing? *Journal of the Geological Society*, *168*(4), 1047–1060. https://doi.org/10.1144/0016-76492010-134

Garreaud, R. D., Molina, A., & Farías, M. (2010). Andean uplift, ocean cooling and Atacama hyperaridity: A climate modeling perspective. *Earth and Planetary Science Letters*, *292*(1–2), 39–50. https://doi.org/10.1016/j.epsl.2010.01.017

Granger, D., Kircher, J., & Finkel, R. (1996). Spatially averaged long-term erosion rates measured from in situ-produced cosmogenic nuclides in alluvial sediment. *The Journal of Geology*, *104*, 249–257.

Hancock, G. S., & Anderson, R. S. (2002). Numerical modeling of fluvial strath-terrace formation in response to oscillating climate. *The Geological Society of America Bulletin*, *114*, 1131–1142.

Hartshorn, K., Hovius, N., Dade, W., & Slingerland, R. (2002). Climate-driven bedrock incision in an active mountain belt. *Science*, *297*(5589), 2036–2038. https://doi.org/10.1126/science.1075078

Hoke, G., Isacks, B., Jordan, T., Blanco, N., Tomlinson, A., & Ramezani, J. (2007). Geomorphic evidence for the post-10 Ma uplift of the western fl ank of the central Andes. *Tectonics*, *26*, TC5021. https://doi.org/10.1029/2006TC002082

Johnson, K. N., & Finnegan, N. J. (2015). A lithologic control on active meandering in bedrock channels. *The Geological Society of America Bulletin*, *127*(11–12), 1766–1776. https://doi.org/10.1130/B31184.1

Kirk-Lawlor, N. E., Jordan, T. E., Rech, J. A., & Lehmann, S. B. (2013). Late Miocene to Early Pliocene paleohydrology and landscape evolution of Northern Chile, 19 degrees to 20 degrees S. *Palaeogeography, Palaeoclimatology, Palaeoecology*, *387*, 76–90. https://doi.org/10.1016/j.palaeo.2013.07.011

Lague, D. (2010). Reduction of long-term bedrock incision efficiency by short-term alluvial cover intermittency. *Journal of Geophysical Research*, *115*, F02011. https://doi.org/10.1029/2008JF001210

Lal, D. (1991). Cosmic ray labeling of erosion surfaces: In situ nuclide production rates and erosion models. *Earth and Planetary Science Letters*, *104*, 424–439.

Langston, A. L., & Temme, A. J. A. M. (2019). Bedrock erosion and changes in bed sediment lithology in response to an extreme flood event: The 2013 Colorado front range flood. *Geomorphology*, *328*, 1–14. https://doi.org/10.1016/j.geomorph.2018.11.015

Langston, A. L., & Tucker, G. E. (2018). Developing and exploring a theory for the lateral erosion of bedrock channels for use in landscape evolution models. *Earth Surface Dynamics*, *6*(1), 1–27. https://doi.org/10.5194/esurf-6-1-2018

Lavé, J., & Avouac, J.-P. (2001). Fluvial incision and tectonic uplift across the Himalayas of central Nepal. *Journal of Geophysical Research*, *106*-B11. 26561–26591.

Lelpi, A., & Lapotre, M. G. A. (2020). A tenfold slowdown in river meander migration driven by plant life. *Nature GeoSciences*, *13*(1), 82+. https://doi.org/10.1038/s41561-019-0491-7

Leopold, L. B., & Maddock, T. J. (1953). The hydrolic geometry of stream channels and some physiographic implications. *U. S. Geological Survey Professional Paper*, *252*, 57.

Li, T., Fuller, T. K., Sklar, L. S., Gran, K. B., & Venditti, J. G. (2020). A mechanistic model for lateral erosion of bedrock channel banks by bedload particle impacts. *Journal of Geophysical Research: Earth Surface*, *125*(6). https://doi.org/10.1029/2019JF005509

Limaye, A. B. (2020). How do braided rivers grow channel belts? *Journal of Geophysical Research: Earth Surface*, *125*(8). https://doi.org/10.1029/2020JF005570

Madella, A., Delunel, R., Akçar, N., Schlunegger, F., & Christl, M. (2018). 10Be-inferred paleo-denudation rates imply that the mid-Miocene western central Andes eroded as slowly as today. *Scientific Reports*, *8*, 2299. https://doi.org/10.1038/s41598-018-20681-x

Malatesta, L., Avouac, J.-P., Brown, N., Breitenbach, S., Pan, J., Chevalier, M.-L., et al. (2018). Lag and mixing during sediment transfer across the tian shan piedmont caused by climate-driven aggradation–incision cycles. *Basin Research*, *30*(4), 613–635.

Malatesta, L., Prancevic, J., & Avouac, J.-P. (2017). Autogenic entrenchment patterns and terraces due to coupling with lateral erosion in incising alluvial channels. *Journal of Geophysical Research: Earth Surface*, *122*(1), 335–355. https://doi.org/10.1002/2015JF003797

May, C., Roering, J., Eaton, L., & Burnett, K. (2013). Controls on valley width in mountainous landscapes: The role of landsliding and implications for salmonid habitat. *Geology*, *41*(4), 503–506. https://doi.org/10.1130/G33979.1

Montgomery, D. (2004). Observations on the role of lithology in strath terrace formation and bedrock channel width. *American Journal of Science*, *304*(5), 454–476. https://doi.org/10.2475/ajs.304.5.454

Montgomery, D., & Gran, W. (2001). Downstream variationsin the width of bedrock channels. *Water Resources Research*, *37*(6), 1841–1846.

Mouchene, M., van der Beek, P., Carretier, S., & Mouthereau, F. (2017). Autogenic versus allogenic controls on the evolution of a coupled fluvial megafan-mountainous catchment system: numerical modeling and comparison with the Lannemezan megafan system (northern Pyrenees, France). *Earth Surface Dynamics*, *5*(1), 125–143. https://doi.org/10.5194/esurf-5-125-2017

Ouimet, W. B., Whipple, K. X., & Granger, D. E. (2009). Beyond threshold hillslopes: Channel adjustment to base-level fall in tectonically active mountain ranges. *Geology*, *37*(7), 579–582. https://doi.org/10.1130/G30013A.1

Portenga, E., & Bierman, P. (2011). Understanding Earths eroding surface with ^{10}Be. *Geological Society of America Today*, *21*(8), 4–10. https://doi.org/10.1130/G111A.1

Schanz, S. A., & Montgomery, D. R. (2016). Lithologic controls on valley width and strath terrace formation. *Geomorphology*, *258*, 58–68. https://doi.org/10.1016/j.geomorph.2016.01.015

Schildgen, T., Balco, G., & Shuster, D. (2010). Canyon incision and knickpoint propagation recorded by apatite 4He/3He thermochronometry. *Earth and Planetary Science Letters*, *293*, 377–387.

Schildgen, T., Hodges, K., Whipple, K., Reiners, P., & Pringle, M. (2007). Uplift of the western margin of the Andean plateau revealed from canyon incision history, southern Peru. *Geology*, *35*, 523–526.

Schlunegger, F., Zeilinger, G., Kounov, A., Kober, F., & Hüsser, B. (2006). Scale of relief growth in the forearc of the andes of northern chile (arica latitude, 18 s). *Terra Nova*, *18*(3), 217–223. https://doi.org/10.1111/j.1365-3121.2006.00682.x

Schumm, S., Mosley, M., & Weaver, W. (1987). *Experimental fluvial geomorphology*. New York, NY: John Wiley and Sons Inc.

Stark, C. P., Barbour, J. R., Hayakawa, Y. S., Hattanji, T., Hovius, N., Chen, H., et al. (2010). The Climatic signature of incised river Meanders. *Science*, *327*(5972), 1497–1501. https://doi.org/10.1126/science.1184406

Starke, J., Ehlers, T. A., & Schaller, M. (2017). Tectonic and climatic controls on the spatial distribution of denudation rates in northern Chile (18 degrees S to 23 degrees S) determined from cosmogenic nuclides. *Journal of Geophysical Research: Earth Surface*, *122*(10), 1949–1971. https://doi.org/10.1002/2016JF004153

Stock, J., Montgomery, D., Collins, B., Dietrich, W., & Sklar, L. (2005). Field measurements of incision rates following bedrock exposure: Implications for process controls on the long profiles of valleys cut by rivers and debris flows. *The Geological Society of America Bulletin*, *117*(1–2), 174–194. https://doi.org/10.1130/B25560.1

Tomkin, J., Brandon, M. T., Pazzaglia, F. J., Barbour, J. R., & Willet, S. D. (2003). Quantitative testing of bedrock incision models for the Clearwater River, NW Washington State. *Journal of Geophysical Research*, *108-B6*, 2308. https://doi.org/10.1029/2001JB000862

Trauerstein, M., Norton, K. P., Preusser, F., & Schlunegger, F. (2013). Climatic imprint on landscape morphology in the western escarpment of the Andes. *Geomorphology*, *194*, 76–83. https://doi.org/10.1016/j.geomorph.2013.04.015

Turowski, J. M. (2020). Mass balance, grade, and adjustment timescales in bedrock channels. *Earth Surface Dynamics*, *8*(1), 103–122. https://doi.org/10.5194/esurf-8-103-2020

Turowski, J. M., Yager, E. M., Badoux, A., Rickenmann, D., & Molnar, P. (2009). The impact of exceptional events on erosion, bedload transport and channel stability in a step-pool channel. *Earth Surface Processes and Landforms*, *34*(12), 1661–1673. https://doi.org/10.1002/esp.1855

Vargas-Luna, A., Duro, G., Crosato, A., & Uijttewaal, W. (2019). Morphological adaptation of river channels to vegetation establishment: A laboratory study. *Journal of Geophysical Research: Earth Surface*, *124*(7), 1981–1995. https://doi.org/10.1029/2018JF004878

Whittaker, A. C., Cowie, P. A., Attal, M., Tucker, G. E., & Roberts, G. P. (2007). Bedrock channel adjustment to tectonic forcing: Implications for predicting river incision rates. *Geology*, *35*(2), 103–106. https://doi.org/10.1130/G20738.1

Wickert, A. D., Martin, J. M., Tal, M., Kim, W., Sheets, B., & Paola, C. (2013). River channel lateral mobility: metrics, time scales, and controls. *Journal of Geophysical Research: Earth Surface*, *118*(2), 396–412. https://doi.org/10.1029/2012JF002386

Yanites, B. J., & Tucker, G. E. (2010). Controls and limits on bedrock channel geometry. *Journal of Geophysical Research*, *115*(F4). https://doi.org/10.1029/2009JF001601

References From the Supporting Information

Arnold, M., Merchel, S., Bourles, D. L., Braucher, R., Benedetti, L., Finkel, R. C., et al. (2010). The French accelerator mass spectrometry facility ASTER: Improved performance and developments. *Nuclear Instruments and Methods in Physics Research Section B: Beam Interactions with Materials and Atoms*, *268*(11–12), 1954–1959. https://doi.org/10.1016/j.nimb.2010.02.107

Braucher, R., Brown, E., Bourlès, D., & Colin, F. (2003). In situ produced ^{10}Be measurements at great depths: implications for production rates by fast muons. *Earth and Planetary Science Letters*, *211*(3–4), 251–258. https://doi.org/10.1016/S0012-821X(03)00205-X

Braucher, R., Guillou, V., Bourles, D. L., Arnold, M., Aumaitre, G., Keddadouche, K., et al. (2015). Preparation of ASTER in-house Be-10/Be-9 standard solutions. *Nuclear Instruments and Methods in Physics Research Section B: Beam Interactions with Materials and Atoms*, *361*, 335–340. https://doi.org/10.1016/j.nimb.2015.06.012

Braucher, R., Merchel, S., Borgomano, J., & Bourlés, D. (2011). Production of cosmogenic radionuclides at great depth: A multi element approach. *Earth and Planetary Science Letters*, *309*, 1–9. https://doi.org/10.1016/j.epsl.2011.06.036

Brown, E. T., Stallard, R. F., Larsen, M. C., Raisebeck, G. M., & Yiou, F. (1995). Denudation rates determined from the accumulation of in situ-produced ^{10}Be in the Luquillo Experimental Forest, Puerto Rico. *Earth and Planetary Science Letters*, *129*, 193–202.

Chmeleff, J., von Blanckenburg, F., Kossert, K., & Jakob, D. (2010). Determination of the Be-10 half-life by multicollector ICP-MS and liquid scintillation counting. *Nuclear Instruments and Methods in Physics Research Section B: Beam Interactions with Materials and Atoms*, *268*(2), 192–199. https://doi.org/10.1016/j.nimb.2009.09.012

Korschinek, G., Bergmaier, A., Faestermann, T., Gerstmann, U. C., Knie, K., Rugel, G., et al. (2010). A new value for the half-life of Be-10 by heavy-ion elastic recoil detection and liquid scintillation counting. *Nuclear Instruments and Methods in Physics Research Section B: Beam Interactions with Materials and Atoms*, *268*(2), 187–191. https://doi.org/10.1016/j.nimb.2009.09.020

Martin, L., Blard, P., Balco, G., Lave, J., Delunel, R., Lifton, N., & Laurent, V. (2017). The CREp program and the ICE-D production rate calibration database: A fully parameterizable and updated online tool to compute cosmic-ray exposure ages. *Quaternary Geochronology*, *38*, 25–49. https://doi.org/10.1016/j.quageo.2016.11.006